Evaluation of radiation force acting on macromolecules by combination of Brownian dynamics simulation with fluorescence correlation spectroscopy

Syoji Ito,[1,2,*] Naoki Toitani,[1] Hiroaki Yamauchi,[1] and Hiroshi Miyasaka[1,†]

[1]*Division of Frontier Materials Science, Graduate School of Engineering Science and Center for Quantum Materials Science under Extreme Conditions, Osaka University, Toyonaka, Osaka 560-8531, Japan*

[2]*PRESTO, Japan Science and Technology Agency (JST), Kawaguchi, Saitama 332-0012, Japan*

(Received 31 March 2010; published 18 June 2010)

The effect of optical gradient force from a focused laser beam on the fluorescence correlation spectroscopy (FCS) was investigated by a computing method based on Brownian dynamics simulation. A series of calculations revealed that, in relatively shallow optical force potential up to $1.0kT_R$ (T_R=298.15 K), the conventional theoretical model of FCS without consideration of the optical gradient force could evaluate the increase in the average number of molecules and the diffusion time in the potential. On the other hand, large deviation between the simulated fluorescence correlation curve and the theoretical model was observed under the potential depth $>1.0kT_R$. In addition, by integrating the optical force potential with the temperature elevation under optical trapping condition, it was deduced that the temperature rise does not seriously affect the average number of particles in the sampling area, but the average residence time is more sensitively affected by the temperature elevation. The present study using the simulation also provides a method to experimentally estimate molecular polarizabilities from FCS measurements.

DOI: 10.1103/PhysRevE.81.061402 PACS number(s): 82.70.−y, 42.50.Wk, 33.50.−j, 33.80.−b

I. INTRODUCTION

In the 19th century, the first experimental detection of radiation force was performed by Lebedev [1]. After the invention of lasers, Ashkin demonstrated microparticle transportation using dispersive force of photons from a laser in 1970 [2] and then developed a single-beam gradient force optical trapping technique (optical tweezers) in 1986 [3]. The trapping method has provided various important applications such as sorting microparticles [4], fabricating colloidal structures [5], determining spring constants for micro-oscillators in microdevices [6], and analyzing interparticle forces [7,8]. Bioscience is one of the fields that have been most benefited from the introduction of optical tweezers. Typical applications include manipulation of DNA conformation [9] and actin filament [10], growth control of neurons [11], and manipulation of living cells [12].

With an increase in the application of optical tweezers, much more tiny particles, i.e., nanoparticles of polymers [13,14], metals [15–17], and *J* aggregates [18], have become the targets of the manipulation. As an approach to the enhancement of radiation force to attain the manipulation of smaller nanoparticles, resonance effects, in addition to the nonresonant conventional optical manipulation, have been also studied. Separation of quantum dots by size using resonant effect was theoretically suggested [19] and experimentally demonstrated in superfluid helium [20]. Osborne *et al.* reported optically biased diffusion of DNA and dye molecules in water at room temperature [21]. Several applications of resonance effects to trapping nanomaterials, such as small fluorophores [22], quantum dots [23], and antibodies [24], have been also reported. The optical trapping also induced the assembling of macromolecules, realizing sphere [25,26] and fiberlike [27] amorphous structures of polymer assembles with characteristic molecular orientations along the polarization of near-infrared (NIR) trapping light.

Although there have been experimental studies to deal with molecular systems using optical tweezers, to our knowledge, no practical method to quantitatively evaluate the mechanical interaction between photons and nanoparticles or molecules in the Rayleigh scattering regime. For a comprehensive analysis of the optical gradient force acting on molecules, fluorescence correlation spectroscopy (FCS) is a promising candidate. FCS was originally proposed by Magde and co-workers in the early 1970s [28–30], and now FCS combined with a confocal laser microscope has become one of the significant techniques for measuring molecular diffusion dynamics and concentration in small spaces [31,32]. However, only handful studies of applications of FCS have been reported to elucidation of optical trapping kinetics. Hosokawa *et al.* [33,34] reported that polymer nanoparticles with 24–200 nm diameters were assembled by radiation force in the potential well, leading to cluster formation depending on the incident laser intensity. The effect of the optical gradient force on the assembling or aggregation dynamics of the nanoparticles was discussed in terms of the average residence time obtained by fluorescence correlation analysis. Theoretically, Meng and Ma proposed an analytical expression of the fluorescence correlation function for nanoparticles in optical gradient field with three-dimensionally spherical symmetric profile [35].

In addition to the gradient optical force, the effect of temperature elevation also affects the molecular diffusion under optical micromanipulation using a NIR laser. In general, focusing of the NIR laser beam into solutions of water and organic solvents causes the elevation of temperature at the focusing area due to the absorption of the NIR light by the solvents. Indeed, we have demonstrated in our recent report

*sito@chem.es.osaka-u.ac.jp

†miyasaka@chem.es.osaka-u.ac.jp

[36] that the thermal motion of fluorescence molecules in solutions of water and several alcohols quickened under irradiation of a focused NIR beam at 1064 nm. This was safely attributed to the elevation of temperature around the focusing area. The result indicates that both trapping effect and temperature rise need to be taken into account for rational understanding of the nanometric optical trapping in solution using FCS.

In order to comprehensively analyze fluorescence correlation signals from FCS measurement for quantitative evaluation of mechanical interaction between photons and molecular systems, it is indispensable to elucidate effects of both optical force potential and temperature elevation. For this purpose, we have employed a numerical simulation based on Brownian dynamics simulation (BDS) method. Computational simulation is a powerful tool to reproduce molecular dynamics driven by the fluctuation in condensed phase; comparing experimental results with simulated ones can elucidate complex and stochastic phenomena. Actually, several reports by using Monte Carlo simulation and BDS [37–39] have been presented for the rational interpretation of experimental results of FCS. In the present study, we have investigated the effect of optical gradient potential on the FCS signals using BDS, and then quantitatively evaluate optical trapping potential acting on molecules.

II. METHODS

Three-dimensional random movements of molecules in solution can be reproduced by the BDS using the algorithm of which bases were developed by Ermak and McCammon [40]. In the BDS, solvent is regarded as a continuum medium, where individual motions of solvent molecules and their specific interactions with solute molecules are not taken into consideration. The time course of the position coordinate for a molecule is expressed by the following algebraic equation:

$$\boldsymbol{r}(t+h) = \boldsymbol{r}(t) + \frac{1}{\xi} h\boldsymbol{f}(t) + \Delta\boldsymbol{r}^B \quad (\xi = 6\pi\eta a). \tag{1}$$

Here, t is the initial time, $\boldsymbol{r}(t+h)$ is the coordinate of the molecule after a short time step h from the time origin, $\boldsymbol{f}(t)$ is the external force acting on the molecule at the time origin, ξ is the viscous drag, and $\Delta\boldsymbol{r}^B$ is the random displacement of Brownian motion. In the present case, the viscous drag ξ is denoted by the viscosity of the solvent, η, and the Stokes radius of the molecule, a, under the assumption that the molecule has spherical shape and the size of the sphere does not change during the Brownian motion. Each component of the random displacement $(\Delta x^B, \Delta y^B, \Delta z^B)$ satisfies the following relations:

$$\langle \Delta x^B \rangle = \langle \Delta y^B \rangle = \langle \Delta z^B \rangle = 0, \tag{2}$$

$$\langle (\Delta x^B)^2 \rangle = \langle (\Delta y^B)^2 \rangle = \langle (\Delta z^B)^2 \rangle = \frac{2kTh}{\xi}. \tag{3}$$

Here, $\langle\ \rangle$ denotes the temporal averaging of the value inside the parentheses, k is the Boltzmann constant, and T is the Kelvin temperature. In the BDS based on the method of Ermak and McCammon, each component of the random displacement, Δi^B $(i=x,y\ z)$, obeys the following normal distribution $\rho(\Delta i^B)$:

$$\rho(\Delta i^B) = \left(\frac{\xi}{4\pi kTh}\right)^{1/2} \exp\left\{-\frac{\xi}{4kTh}(\Delta i^B)^2\right\}. \tag{4}$$

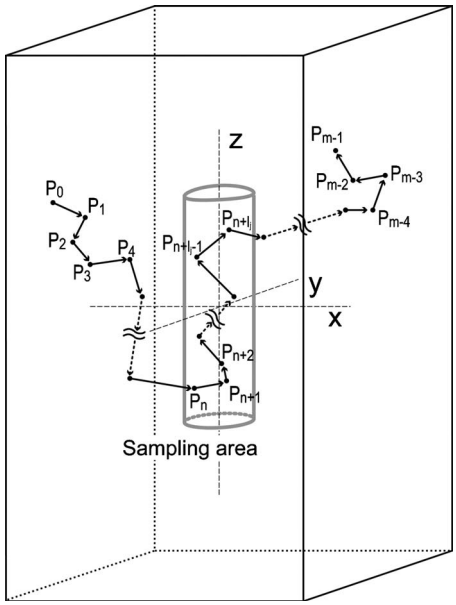

FIG. 1. A schematic illustration of the movement of a molecule in the present simulation.

In the present study, the random movement of a molecule was calculated in such a manner that the long-time statistical distribution of the random walk obeys the distribution function denoted by Eq. (4). Figure 1 schematically illustrates the configuration of the present simulation for the ith molecule. The molecule randomly moves step by step from the initial point P_0 to the last point P_{m-1}; here, m is the total number of the steps in one simulation process, which should be enough large for the reproduction of the stochastic phenomenon. During the m-times displacements, the molecule sometimes stays in the sampling area of a confocal microscope (the cylindrical area in the figure).

For the reproduction of actual FCS measurements, the frequency of photon emission from a molecule is set to be proportional to the intensity of excitation laser light in the following manner. In the present simulation, a three-dimensional Gaussian profile is employed as the excitation light intensity distribution as expressed by Eq. (5),

$$I_{\mathrm{exc}}(r,z) = I_0 \exp\left(-\frac{2r^2}{R_{e\_xy}^2} - \frac{2z^2}{R_{e\_z}^2}\right) \quad (r^2 = x^2 + y^2). \tag{5}$$

Here, R_{e_z} and R_{e_xy} are, respectively, the sizes of beam waist in the direction of the propagation of laser light (z axis) and in the perpendicular direction (x and y axes).

At the same time, we consider the gradient force acting on molecules in the optical force potential. The shape of the potential well with Gaussian distribution is expressed by Eq. (6),

$$U_{\text{trap}}(r,z) = -U_0(I)\exp\left(-\frac{2r^2}{R_{xy}^2}-\frac{2z^2}{R_z^2}\right) \quad (r^2 = x^2 + y^2). \tag{6}$$

Here, U_0 is the depth of the potential, I is the incident laser power, and R_z and R_{xy} are the sizes of beam waist in the direction of the propagation of the laser light (z axis) and in the perpendicular direction (x and y axes). In the typical experimental condition of FCS where the excitation laser light is focused with the spot size comparable to its wavelength, the ratio of R_{xy} to R_z has been determined as 0.2 in typical experiments of FCS with visible excitation light sources. Hence, we set $R_{xy}/R_z=0.2$ as the focusing condition of a laser beam for optical trapping in the present simulation. The amplitude and the direction of the gradient force are obtained by calculating the derivative of Eq. (6) at the positional coordinate of the molecule.

We have used following values as parameters in the present series of simulation: $R_{e\_xy}=0.25$ μm as the beam waist (radius) of excitation light, $R_{xy}=0.5$ μm as the beam waist of trapping light, and 50 ns as the time step for the BDS. In addition, we set the boundary condition that molecules move around in a rectangular-solid area with 5×5 μm^2 area of base and 10 μm height. The viscosity of the solvent was set to that of water, of which temperature dependence was measured with an Ostwald viscometer [36].

We have evaluated the effect of temperature elevation due to the absorption of NIR trapping laser by solvent (water) as well as the effect of optical gradient force on FCS signals. As a parameter necessary for the series of simulations, the temperature elevation coefficient ϕ_{water} (K/W) under the optical trapping condition with Nd^{3+}:YAG laser was experimentally evaluated to be ~24 K/W in our recent report [36]. Because viscosities of solvents alter with temperature, the relation between viscosity and temperature is necessary for the series of simulations. In the present study, we have used our experimental data of water described above (see Ref. [36] for more details). Simulations were carried out under the condition that temperature had uniform spatial distribution and the temperature elevation ΔT is proportional to the incident laser power I as expressed by Eq. (7) [36],

$$\Delta T = \phi_{\text{water}} I. \tag{7}$$

We also assumed the linear dependence of the depth of the optical force potential U_0 on the incident laser power I as expressed by Eq. (8),

$$U_0(I) = \sigma I. \tag{8}$$

Here, σ (kT_R/W) is a coefficient relating to the optical force potential and the incident power, and this value is, in actual calculations, a function of the polarizability of the molecule.

In the actual calculation, we obtained autocorrelation curves of the simulated results in the following manner. First, we calculated molecular movements under the optical force potential as described above. Second, we counted photons emitted from the molecule in the confocal volume (sampling area in Fig. 1). In the correcting procedure, we assumed that the fluorescence molecule emits photons with the probability p_F. In other words, the fluorescence lifetime of the dye (typically, several nanoseconds) was not taken into consideration. This is because the bin time of the present simulation, 200 ns, is much longer than fluorescence lifetimes of typical dyes. The value of p_F was chosen, so that the photon-counting rate, a number of photons counted in a unit time, was comparable to that in the typical experimental condition, such as 10 000–100 000 counts/s. The number of photons counted in every 200 ns time window was thus obtained as a function of the time course in the simulation. Finally, fluorescence autocorrelation curves were provided by calculating the autocorrelation function of the time courses of fluorescence fluctuation in the sampling area.

III. ANALYSIS

The autocorrelation function $G(\tau)$ of the raw data of FCS, fluorescence intensity vs time course of measurement, is usually employed for quantitative analysis. $G(\tau)$ of fluorescence fluctuation at the confocal volume is analytically derived by the following equation [31,32]:

$$G(\tau) = 1 + \frac{1}{N}\left(1+\frac{\tau}{\tau_D}\right)^{-1}\left(1+\frac{\tau}{w^2\tau_D}\right)^{-1/2}, \tag{9}$$

where τ is the dimensionless time normalized by 1 ms ($\tau=t/1$ ms), N is the average number of molecules in the confocal volume V_{conf} with cylindrical shape, and w is the structure parameter defined by $w=w_z/w_{xy}$. Here, w_z and w_{xy} are, respectively, the axial length and radial radii of the cylindrical confocal volume ($V_{\text{conf}}=2pw_z w_{xy}^2$). τ_D is the average residence time related to the translational diffusion coefficient D by Eq. (9),

$$\tau_D = \frac{w_{xy}^2}{4D}. \tag{10}$$

The analysis of the autocorrelation function using Eq. (9) provides the average residence time τ_D and the average number of molecules in the confocal volume. It should be noted for clarity that the analytical model of Eq. (9) is derived on the assumption that molecules undergo the translational diffusion in homogeneous media without any external field. That is, the optical trapping potential is not taken into consideration in the model of Eq. (9).

IV. RESULTS AND DISCUSSION

A. Effect of optical gradient force on fluorescence correlation curves

Figure 2(a) shows an autocorrelation function calculated from the fluorescence intensity trajectory obtained by the simulation without optical gradient force under the following condition: temperature of 297.85K, viscosity of 0.8963 cP (water), and hydrodynamic diameter of molecule of 2 nm. The autocorrelation curve was well fitted by the conventional analytical model expressed with Eq. (9). The diffusion coefficient derived from the analysis was 2.4×10^{-10} m^2 s^{-1}, of which value is almost identical to that initially set for the simulation (2.3×10^{-10} m^2 s^{-1}). In addition, we confirmed

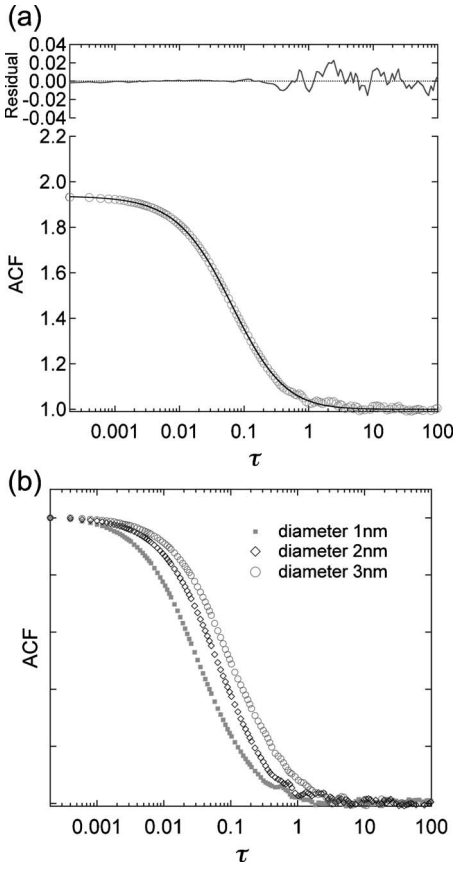

FIG. 2. (a) An autocorrelation function curve of molecules with a diameter of 2.0 nm in water obtained from the present simulation with its fitting curve based on Eq. (12) and the residual. (b) Autocorrelation function curves of molecules with diameters of 1.0, 2.0, and 3.0 nm in water obtained from the present simulation.

the validity of the simulation by changing the hydrodynamic diameter of molecules as a parameter. Figure 2(b) shows the autocorrelation curve for the simulated results, indicating that the correlation curve decays rapidly with increasing hydrodynamic diameter. τ_D obtained by the analysis with Eq. (9) was confirmed to be in linear proportion to the hydrodynamic diameter, as predicted from Eq. (10). These results indicate that the present simulation method can be applied to the quantitative evaluation of the FCS experiments,

$$\frac{kT}{6\pi\eta a} = D = \frac{w_{xy}^2}{4\tau_D}. \tag{11}$$

Figure 3 shows autocorrelation curves for molecules with a hydrodynamic diameter of 2.5 nm in water at temperature T_R (=298.15K) in the presence of the optical trapping potential, of which depth β ranges from 0.1 to 4.0. Here, β is a dimensionless expression of optical trapping potential defined by Eq. (12),

$$\beta = \frac{U_0}{kT_R}. \tag{12}$$

Solid lines in the figures [Figs. 3(a)–3(h)] are results analyzed on the basis of the conventional model of FCS [Eq.

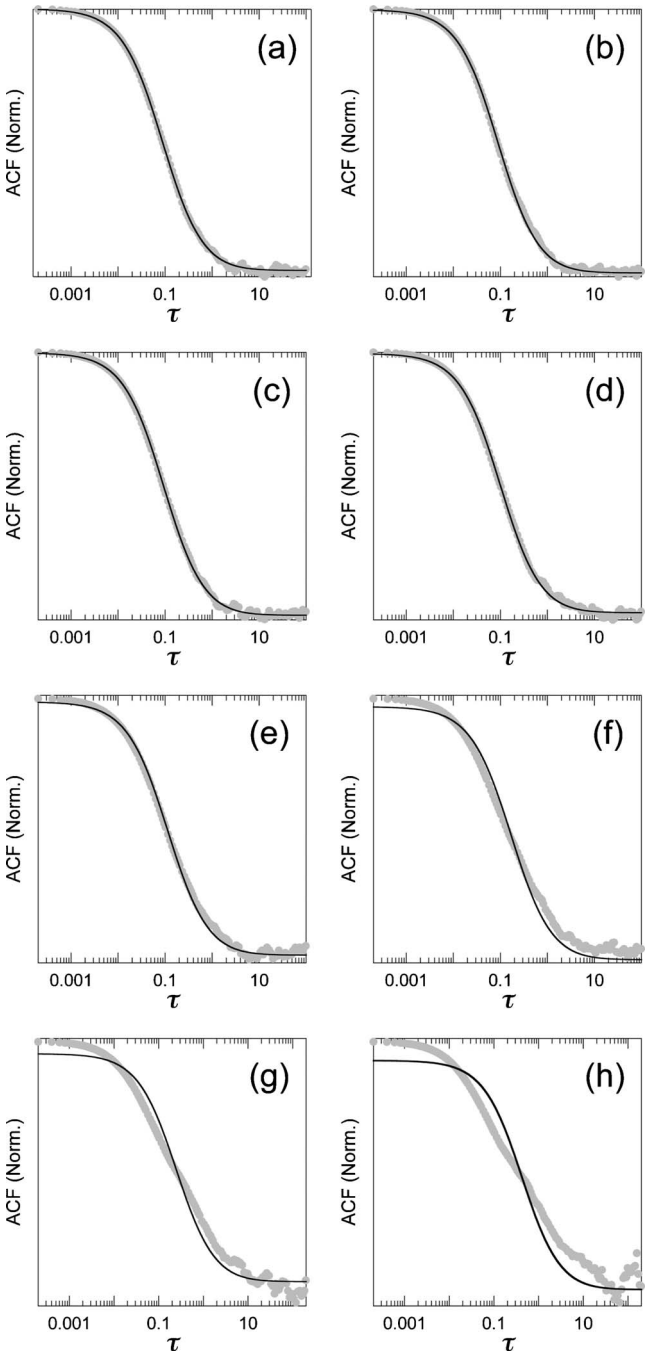

FIG. 3. Fluorescence autocorrelation curves (gray solid circles) in the presence of optical gradient field with fitting results (solid lines) on the basis of Eq. (8). The depths of the potential, β, are (a) 0, (b) 0.2, (c) 0.5, (d) 0.8, (e) 1.0, (f) 2.0, (g) 3.0, and (h) 4.0.

(9)]. Because the analytical model of Eq. (9) does not take any external field into account, the results are not "true values" but approximate ones. However, the analysis indicates that the effect of the optical gradient force is overall negligible up to the potential depth of β=0.8. In other words, the autocorrelation curves are well reproduced by using the conventional analytical model [Eq. (9)] in relatively shallow trapping potential. In the presence of the optical force potential of which depth is deeper than $1.0kT_R$ ($\beta > 1.0$), the conventional analytical model no longer reproduces the au-

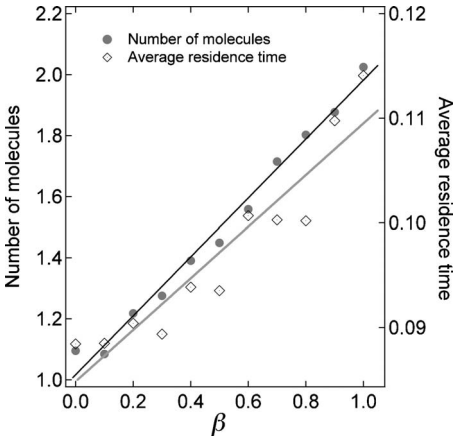

FIG. 4. Plot of the number of molecules N and the average residence time τ_D in the sampling volume as functions of the optical force potential depth in the range of $0 \leq \beta \leq 1.0$ with fitting results (solid lines) on the basis of Eqs. (14) and (15).

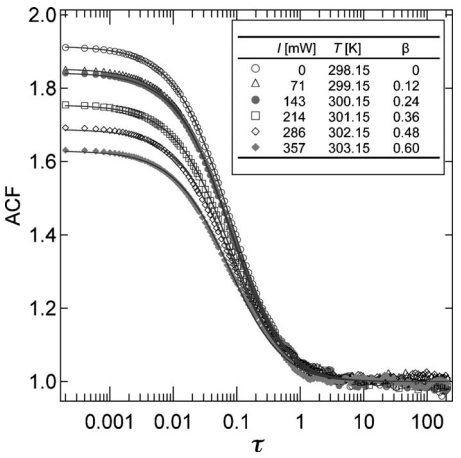

FIG. 5. Fluorescence autocorrelation curves obtained by the simulation taking into account both optical gradient force and temperature elevation under the condition of $\sigma = 1.7kT_R/\mathrm{W}$ and $\phi_{\mathrm{water}} = 24$ K/W. Temperature T and the depth of the optical force potential, β, are summarized in the inset with the corresponding incident laser power I.

tocorrelation curves obtained through the computational simulation. The deviation between the curve based on Eq. (9) and the simulation results becomes pronounced with increasing depth of the optical gradient potential. From these results we can conclude that the conventional analytical model of FCS is applicable to the analysis of fluorescence autocorrelation curves under relatively shallow optical gradient potential up to approximately $\beta \sim 1.0$, while a new approach is required in the region with deep potential $\beta \geq 1.0$.

In other words, although the effect of radiation force on molecular diffusivity is rather small in the region $\beta \lesssim 1$, the number of molecules and the average residence time may be affected. Figure 4 shows dependences of the number of molecules and the average residence time of molecules in the confocal volume under the radiation force potential from 0 to kT_R. This figure clearly indicates that the optical force potential actually affects these two values even in this relatively shallow region of the potential; the two values almost linearly increase with an increase in the potential depth.

The theoretical expressions of τ_D modified by optical trapping potential have been derived by Osborne *et al.* [21] and Chirico *et al.* [22] as Eq. (13),

$$\tau_D \approx \tau_0 \exp\left(\frac{U_0}{kT_R}\right) \approx \tau_0(1+\beta). \tag{13}$$

Here, τ_0 is the average residence time without optical trapping potential. Although Eq. (13) predicts that the values of τ_D become double in the case $\beta = 1.0$, the effect of the trapping potential on τ_D is smaller in the present simulation than that from the prediction. This is probably because the spot size of the trapping beam is larger than that of the excitation light. However, the simulated result can be approximately analyzed with Eq. (14) as shown in Fig. 4. The fitting parameter A should be related to the shape of the trapping potential and the excitation spot size,

$$\tau_D \approx \tau_0(1+A\beta) \quad (\beta < 1). \tag{14}$$

At the same time, the present simulation result of the average number of molecules, N, is also well reproduced by the following equation [Eq. (15)]; the value of N linearly increases with an increase in the trapping potential and the value doubles at the potential depth of $\beta = 1.0$ $(1.0kT_R)$,

$$N \approx N_0(1+B\beta) \quad (\beta < 1). \tag{15}$$

Here, N_0 is the average number of molecules without optical trapping potential and B is a fitting parameter having the similar role of the fitting parameter A.

B. Effect of temperature elevation under optical trapping condition

In addition to the "trapping" effect by the radiation force, it is necessary for the precise analysis to take into account the effect of the temperature increase by the trapping laser light. Indeed, the temperature elevation is quite effective in a number of actual experimental systems where NIR laser is employed as an optical tweezing in solutions of water and many sorts of organic solvents [36]. Hence, the effect of temperature elevation has been taken into consideration. Figure 5 shows autocorrelation function curves obtained by the simulation under the condition that $\sigma = 1.7kT_R/\mathrm{W}$ and $\phi_{\mathrm{water}} = 24$ K/W. Similar to the result shown in Fig. 3, autocorrelation function curves obtained from the series of simulations could be analyzed by the analytical model of Eq. (9) up to the potential depth of $\beta = 1.0$. As is clearly shown in Fig. 5, the temporal origin of the autocorrelation curve, $G(10^{-6})$, decreased with an increase in the incident laser power; this is safely attributed to the increase in the average number of molecules in the confocal area by radiation force as was already shown in Fig. 4.

Dependences of the average number of molecules N and the average residence time τ_D on the incident laser power for optical tweezing under various conditions of σ were obtained through a series of simulations. Representative results are shown in Fig. 6. The value of N exhibited linear dependence on the incident laser power in the region of σ examined in

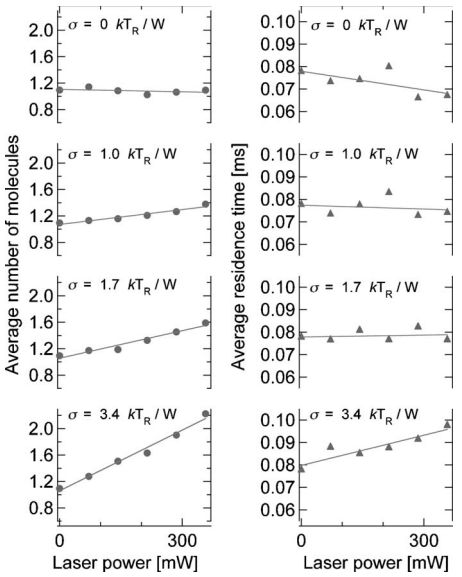

FIG. 6. Dependences of the average number of molecules N (left) and the average residence time τ_D (right) on the incident laser power under conditions of σ. Values of σ are indicated in the plots.

the present study $(0-10kT_R/\mathrm{W})$. With increasing value of σ, the slope for N versus incident laser power became larger monotonously. On the other hand, the average residence time slightly decreased with an increase in the incident laser power under the condition of $\sigma \sim 0$. This is due to the thermal motion promoted by the temperature elevation as already demonstrated in our previous report [36]. This effect was, however, overcome by the effect of optical gradient field (optical trapping potential) at $\sigma \gtrsim 1.7kT_R/\mathrm{W}$ as shown in the right part of Fig. 6.

C. Evaluation of optical gradient force potential in terms of N from FCS measurement

As already shown in Figs. 4 and 6, N in the focusing area of the trapping laser light exhibited almost linear dependence on the depth of the optical force potential, indicating that we can parametrize the effect of the optical gradient field in terms of the average number of molecules in the sampling area of the confocal microscope. As representatively shown in Fig. 1, a molecule in the simulation randomly moves step by step from the initial point P_0 to the last point P_{m-1}. During the m-times displacements, the molecule sometimes comes in the sampling area, for example, l_j steps between points of P_n and P_{n+lj} in Fig. 1. Under the actual condition of the present simulation, one molecule passed through the sampling area many times during one simulation process; the total number of steps where the ith molecule was in the sampling volume, M_i, is obtained by summing up l_j as denoted by Eq. (16),

$$M_i = \sum_j l_j \tag{16}$$

The average number of molecules in the sampling area, N_{hist}, is obtained by summation of M_i/m_i for all molecules as expressed by Eq. (17).

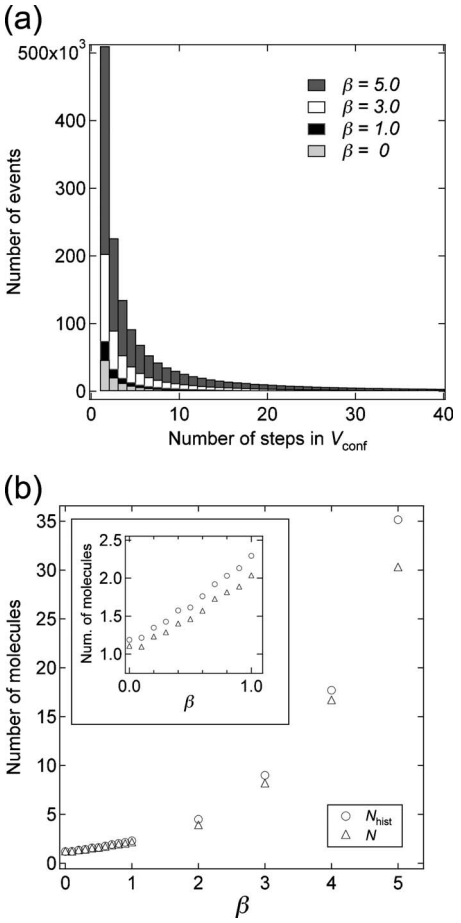

FIG. 7. (a) Histograms for the number of steps in the sampling volume of FCS with and without optical gradient field; the values of the potential depth are expressed in the figure. (b) Plots of N and N_{hist} as functions of the potential depth of induced optical gradient field.

$$N_{\mathrm{hist}} = \sum_i \frac{M_i}{m_i} \tag{17}$$

By comparing N obtained by the analysis on the basis of Eq. (9) with N_{hist}, we can evaluate the applicability of the analytical method based on Eq. (9) to FCS signals in the presence of optical gradient field.

Figure 7(a) shows the histogram of the number of steps for the molecules staying inside the sampling area under the optical force potential with $1.0kT_R$, $2.0kT_R$, and $5.0kT_R$ and without the potential. The histograms clearly indicate that the summation of M_i increased with an increase in the potential depth. This result is consistent with the increase in the number of molecules along with the optical force potential depth as already shown in Figs. 4 and 6. N and N_{hist} are plotted as functions of the optical force potential depth in Fig. 7(b). In the region of the potential depth up to $\sim 1.0kT_R$, the values of N and N_{hist} exhibit good agreement. This ensures that the florescence autocorrelation curves for molecules under relatively shallow optical gradient potential were well analyzed by the analytical model expressed by Eq. (9). That is, the effect of the optical force potential in the region from $0.2kT_R$

to $1.0kT_R$ is detectable using FCS as in Fig. 4, while the potential does not seriously affect the shape of the fluorescence autocorrelation function. On the other hand, in the presence of the optical force potential $>1.0kT_R$, the fluorescence correlation curves were no longer reproduced by the analytical model of Eq. (9) as shown in Fig. 3. Indeed, the deviation between N and N_{hist} is pronounced with an increase in the induced potential depth as shown in Fig. 7(b). From these results, we can conclude that the analytical method on the basis of Eq. (9) can be used for evaluating the effect of the optical force potential up to $\sim 1.0kT_R$.

D. Estimation method of the depth of optical gradient potential acting on molecules in solution

The present simulation also enables us to evaluate the depth of optical gradient potential acting on molecules through the molecular polarizability from experimental results of FCS in solutions. As shown in Fig. 8, the increasing rate of N as a function of incident laser power at 1064 nm is approximately proportional to the parameter σ in the relatively shallow optical force potential (up to $\sim kT_R$). Hence, one can estimate the value of σ for actual molecular systems in water by experimentally obtaining the number of molecules through FCS measurements. From the simple theoretical model of the optical trapping where a molecule is approximated as a point dipole, the depth of the optical force potential can be expressed by Eq. (18),

$$U_0 = \frac{n_m \alpha}{c} I. \tag{18}$$

Here, n_m is the refractive index of water, c is the speed of light, and α is the polarizability of a molecule. Combining Eqs. (8) and (18), we obtain the following approximated relation:

$$\sigma \cong \frac{n_m \alpha}{c}. \tag{19}$$

In this way, the potential depth of the optical gradient force and the polarizability of a molecule can be estimated from experimental results of FCS.

V. SUMMARY

We have investigated the effect of optical gradient field on autocorrelation curves of FCS using the computational simulation method developed on the basis of BDS. The fluorescence autocorrelation curves for molecules under relatively shallow potential up to $\sim 1.0kT_R$ could be approximately analyzed by the standard analytical model of FCS [Eq. (9)], while in the presence of the potential $>1.0kT_R$, the autocorrelation curves were no longer reproduced by the analytical model. This result could determine the limit of the analysis using the analytical model of Eq. (9). The series of simulations taking into account temperature elevation due to the absorption of the trapping laser beam have clarified that the temperature elevation did not seriously affect the average number of molecules in the sampling area. On the other hand the average residence time was more sensitively affected by the temperature elevation. The present approach can lead to rational understanding of the mechanical interaction between molecules and photons and its resultant effects on FCS signals. We have also developed a method to estimate polarizability of molecules from FCS measurements under the experimental condition that gradient force potential depth is lower than the average thermal energy at room temperature.

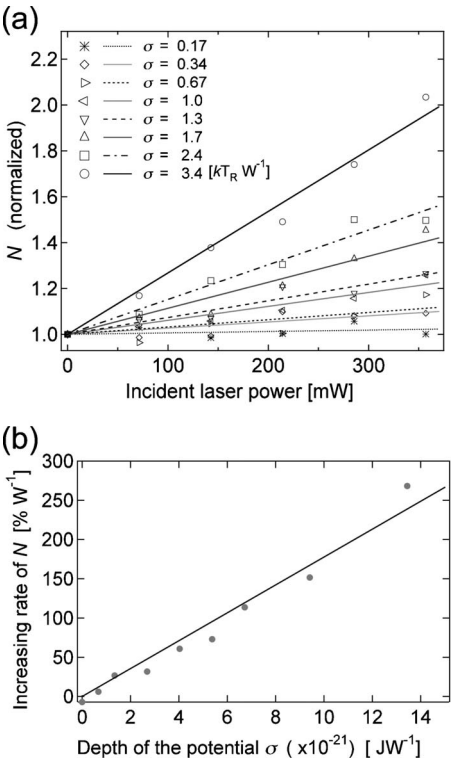

FIG. 8. (a) Dependences of number of molecules N (normalized) on the incident laser power for various σ values with corresponding linear curves obtained by the least-squares method. (b) Plot of the increasing rate of N (normalized) as a function of the depth of optical force potential, σ, obtained from the result shown in (a).

[1] P. N. Lebedew, Ann. Phys. (Leipzig) **6**, 433 (1901).
[2] A. Ashkin, Phys. Rev. Lett. **24**, 156 (1970).
[3] A. Ashkin, J. M. Dziedzic, J. E. Bjorkholm, and S. Chu, Opt. Lett. **11**, 288 (1986).
[4] M. P. MacDonald, G. C. Spalding, and K. Dholakia, Nature (London) **426**, 421 (2003).
[5] A. Terray, J. Oakey, and D. W. M. Marr, Appl. Phys. Lett. **81**, 1555 (2002).
[6] S. Kawata, H.-B. Sun, T. Tanaka, and K. Takada, Nature (London) **412**, 697 (2001).

[7] J. C. Crocker and D. G. Grier, Phys. Rev. Lett. **73**, 352 (1994).
[8] J.-C. Meiners and S. R. Quake, Phys. Rev. Lett. **82**, 2211 (1999).
[9] S. B. Smith, Y. Cui, and C. Bustamante, Science **271**, 795 (1996).
[10] K. Kitamura, M. Tokunaga, A. H. Iwane, and T. Yanagida, Nature (London) **397**, 129 (1999).
[11] A. Ehrlicher, T. Betz, B. Stuhrmann, D. Koch, V. Milner, M. G. Raizen, and J. Käs, Proc. Natl. Acad. Sci. U.S.A. **99**, 16024 (2002).
[12] A. Ashkin, J. M. Dziedzic, and T. Yamane, Nature (London) **330**, 608 (1987).
[13] S. Ito, H. Yoshikawa, and H. Masuhara, Appl. Phys. Lett. **78**, 2566 (2001).
[14] S. Ito, T. Mizuno, H. Yoshikawa, and H. Masuhara, Jpn. J. Appl. Phys., Part 2 **43**, L885 (2004).
[15] K. Svoboda and S. M. Block, Opt. Lett. **19**, 930 (1994).
[16] S. Ito, H. Yoshikawa, and H. Masuhara, Appl. Phys. Lett. **80**, 482 (2002).
[17] S. Ito, T. Mizuno, H. Yoshikawa, and H. Masuhara, Jpn. J. Appl. Phys., Part 2 **46**, L241 (2007).
[18] Y. Tanaka, H. Yoshikawa, and H. Masuhara, J. Phys. Chem. B **110**, 17906 (2006).
[19] T. Iida and H. Ishihara, Phys. Rev. Lett. **90**, 057403 (2003).
[20] K. Inaba, K. Imaizumi, K. Katayama, M. Ichimiya, M. Ashida, T. Iida, H. Ishihara, and T. Itoh, Phys. Status Solidi B **243**, 3829 (2006).
[21] M. A. Osborne, S. Balasubramanian, W. S. Furey, and D. Klenerman, J. Phys. Chem. B **102**, 3160 (1998).
[22] G. Chirico, C. Fumagalli, and G. Baldini, J. Phys. Chem. B **106**, 2508 (2002).
[23] L. Pan, A. Ishikawa, and N. Tamai, Phys. Rev. B **75**, 161305(R) (2007).
[24] H. Li, D. Zhou, H. Browne, and D. Klenerman, J. Am. Chem. Soc. **128**, 5711 (2006).
[25] P. Borowicz, J. Hotta, K. Sasaki, and H. Masuhara, J. Phys. Chem. B **101**, 5900 (1997).
[26] J. Hofkens, J. Hotta, K. Sasaki, H. Masuhara, T. Taniguchi, and T. Miyashita, J. Am. Chem. Soc. **119**, 2741 (1997).
[27] S. Masuo, H. Yoshikawa, H.-G. Nothofer, A. C. Grimsdale, U. Scherf, K. Müllen, and H. Masuhara, J. Phys. Chem. B **109**, 6917 (2005).
[28] D. Magde, E. L. Elson, and W. W. Webb, Phys. Rev. Lett. **29**, 705 (1972).
[29] E. L. Elson and D. Magde, Biopolymers **13**, 1 (1974).
[30] D. Magde, E. Elson, and W. W. Webb, Biopolymers **13**, 29 (1974).
[31] For example, *Fluorescence Correlation Spectroscopy*, Springer Series in Chemical Physics No. 65, edited by R. Rigler and E. S. Elson (Springer, Berlin, 2001).
[32] O. Krichevsky and G. Bonnet, Rep. Prog. Phys. **65**, 251 (2002).
[33] C. Hosokawa, H. Yoshikawa, and H. Masuhara, Jpn. J. Appl. Phys., Part 2 **45**, L453 (2006).
[34] C. Hosokawa, H. Yoshikawa, and H. Masuhara, Phys. Rev. E **72**, 021408 (2005).
[35] F. Meng and H. Ma, J. Phys. Chem. B **109**, 5580 (2005).
[36] S. Ito, T. Sugiyama, N. Toitani, G. Katayama, and H. Miyasaka, J. Phys. Chem. B **111**, 2365 (2007).
[37] M. Huertas de la Torre, R. Forni, and G. Chirico, Eur. Biophys. J. **30**, 129 (2001).
[38] J. A. Dix, E. F. Y. Hom, and A. S. Verkman, J. Phys. Chem. B **110**, 1896 (2006).
[39] T. Wocjan, J. Krieger, O. Krichevsky, and J. Langowski, Phys. Chem. Chem. Phys. **11**, 10671 (2009).
[40] D. L. Ermak and J. A. McCammon, J. Chem. Phys. **69**, 1352 (1978).